University of Pardubice
Faculty of Chemical Technology
Department of Physical Chemistry

Mgr. Mariia Lemishka

Binuclear transition metal ion centers in zeolites: Their preparation, characterization, and catalytic properties.

Theses of Doctoral Dissertation

Supervisor: Mgr. Jiří Dědeček, CSc., DSc.
Supervisor-consultant: Doc. Mgr. Edyta Anna Tabor, Ph.D.
Supervisor-consultant: Doc. Ing. Zdeněk Sobalík, CSc.

Pardubice 2024

Study program: **Physical Chemistry**

Study field: **Physical Chemistry**

Author: **Mariia Lemishka**

Supervisor: **Mgr. Jiří Dědeček, CSc., DSc.**

Year of the defense: **2024**

References

Mariia Lemishka. *Binuclear transition metal ion centers in zeolites: Their preparation, characterization, and catalytic properties.* Pardubice, 2024. 149 pages. Dissertation thesis (Ph.D.). University of Pardubice, Faculty of Chemical Technology, Department of Physical Chemistry. J. Heyrovský Institute of Physical Chemistry of the CAS, v. v. i. Supervisor Mgr. Jiří Dědeček, CSc., DSc.

Contents

Abstract

Transition metal ion (TMI)-exchanged zeolites have shown excellent activity and selectivity in the oxidation of methane (CH_4) to methanol (CH_3OH) at room temperature (RT). Therefore, a detailed understanding of the structure-activity-stability relationship for their use in the reaction is required. In this thesis, newly developed (reported for the first time) TMI-based Fe(II)-, Co(II)-, Ni(II)-, and Mn(II)-ferrierite (FER) along with Fe(II)-mordenite (MOR) zeolite catalysts are presented for molecular oxygen (O_2) and nitrous oxide (N_2O) splitting for the selective oxidation of CH_4 towards CH_3OH. In addition, experimental and theoretical methods were applied to investigate the O_2 and N_2O activation over the presented metallozeolites. This research has confirmed the formation of highly reactive species called alpha oxygen (α-O) and their reactivity in CH_4 oxidation. The theoretical study of O_2 activation was also extended to Fe(II)-beta (*BEA) and Fe(II)-Linde Type A (LTA) zeolites.

The first part of this thesis focuses on explaining the methodology, which was based on a combination of several techniques, such as in-situ Fourier-transform infrared spectroscopy (FTIR), X-ray absorption near-edge structure (XANES), Mössbauer, ultraviolet-visible spectroscopy (UV-Vis), mass spectrometry, FTIR analysis in the gas phase, and density functional theory (DFT) calculations used to study the formation, stabilization, evolution, and reactivity of α-O from O_2 cleavage over Fe-FER, and following treatment with CH_4.

In the study, special attention was dedicated to analyzing the stabilization, siting, and location of bare divalent cations of Fe, Co, Ni, and Mn in the extra-framework cationic positions in the FER matrix. In addition, the unique type of active (binuclear) centers was investigated in the TMI-based FERs, which is the crucial point for subsequent treatment with O_2 or N_2O and CH_4. Also, the potential of zeolites (MOR, *BEA, and LTA) other than the FER matrix was evaluated in order to find an arrangement suitable for the formation of an optimal distance between two divalent metal (M(II)) ions (binuclear center formation), which could cooperate in O_2 dissociation. Additionally, the aluminum (Al) distribution was studied in MOR zeolite.

The following sections are devoted to the investigation of the potential for O_2 activation and the following CH_4 selective oxidation over Co(II), Ni(II), and Mn(II) in the FER matrix. The formation of α-O, obtained by N_2O decomposition and its activity toward CH_4 to CH_3OH oxidation, was studied over the binuclear centers of Fe(II), Co(II), and Ni(II)-FERs. Finally, the influence of zeolite topology on the catalytic performance in catalytic reduction (CR_{N2O}) and selective catalytic reduction (SCR_{N2O}) reactions over Fe(II)-FER and Fe(II)-MOR with similar Fe(II) loadings was investigated.

Keywords

Alpha oxygen, Ferrierite, Heterogeneous Catalysis, Infrared spectroscopy, Methane, Methanol, Molecular oxygen, Mordenite, Selective oxidation of methane to methanol, Transition metal ion sites, Zeolite.

I Introduction

1.1 Transition metal ion extra-framework sites in the metallozeolites and aluminum distribution

Zeolites represent one of the most important groups of heterogeneous industrial catalysts.[1, 2] The outstanding catalytic properties of zeolite catalysts result from a unique combination of their chemical composition and structure. Zeolites are crystalline microporous aluminosilicates built from silicate (SiO_4) and aluminate (AlO_4^-) tetrahedra that share corners to form a regular channel/cavity system.[3] The isomorphous substitution of aluminum (Al) in the SiO_4 framework induces a negative framework charge, which can be balanced by two types of extra-framework cationic species – the protons involved in Brønsted acid sites (Si-OH-Al) represent active sites in acid-catalyzed reactions and bare cations and metal-oxo species serve as the active sites in redox catalyzed processes.[4]

Zeolites can be divided into two main categories depending on the amounts of silicon (Si) and Al atoms in the framework.[5] The Si-rich zeolites, which are characterized as materials with a Si/Al molar ratio > 5 (e.g., FER, MOR, Mobil-type five (MFI), and beta (*BEA) zeolites), include the pentasil zeolite family, where the SiO_4 structure composed of pentagonal arrangements of atoms. By contrast, Al-rich zeolites are considered to have a matrix with Si/Al < 5, and the most common zeolites in this category are Lynde type A (LTA), *BEA zeolite or chabazite (CHA) frameworks. The organization of Al atoms in the zeolites controlled the stabilization of catalytically active centers (both protons and TMI centers) through Al atom concentration, location, and distances in the zeolite matrix. It was experimentally proven that in Si-rich FER, MFI, and MOR zeolites, Al atoms can be organized as exclusively Al pairs (Al-O-(Si-O)$_2$-Al) or single Al atoms.[5] In contrast, in Al-rich *BEA zeolite, except for single Al atoms and Al pairs, Al-O-Si-O-Al sequences and close unpaired Al atom (Al-O-(Si-O)$_3$-Al) are observed. Furthermore, in Al-rich LTA zeolite, the Al-O-Si-O-Al sequences are predominated.

The organization of Al atoms in the zeolite plays a crucial role in the stabilization of various types of ion/oxo species in metallozeolites. It was confirmed that the introduction of TMIs to the zeolite led to the formation of several types of counter metal (M) (ion/oxo species: bare cations (balancing negative zeolite charge) coordinated to four oxygen atoms of the framework, cation-oxo species, bi(poly) nuclear cation-oxo species, metal (ion(oxo)) clusters, or metal oxide species.[6]

The research presented in this thesis is focused on analyzing the formation, cooperation, and redox behavior of bare cations located in the cationic positions of FER, MOR, *BEA, and LTA zeolites. For the first time, in MOR topology, Wichterlova et al.[7] have spectroscopically (UV-Vis and FTIR spectroscopy studies) confirmed the existence of three cationic positions indicated as α, β, and γ that differ in the symmetry and the location in zeolite matrix (Fig. 1.). They showed that the divalent cations sitting in α cationic positions of MOR are located above the center of 6-MRs and coordinated to four oxygen atoms. In the β cationic site in MOR, distinguished as the most populated fraction, the divalent cations are coordinated to four oxygen atoms of the 8-MR and exhibit a planar geometry. In the γ cationic position (a less occupied), divalent cations are stabilized in a closed coordination sphere with pseudo-octahedral coordination.

Experimental study (FTIR, UV-VIS, Mössbauer, and MAS-NMR) results supported by DFT calculation revealed that the symmetry and the location of α, β, γ cationic positions are similar in FER and *BEA zeolites to those described above cationic positions in MOR.[23, 25]

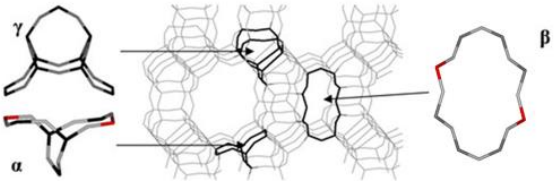

Fig. 1. Local framework structures of the α, β, and γ sites in the MOR zeolite. Al atoms are in red, silicon atoms are in black, and oxygen atoms are in grey.

1.2 Methane: Its properties and utilization

From an economic and environmental perspective, there has been a great deal of interest in the chemical utilization of CH_4.[8, 9]. Methane, being a main component of natural gas, represents the cheapest and most abundant source of hydrocarbons. However, its chemical features, such as low polarizability and high carbon-hydrogen (C-H) bond strength (439 kJ/mol), make it highly resistant to transformation. Nevertheless, it was shown that for CH_4 conversion the presence of the catalysts is needed. The role of the catalyst in the process of formation of oxygenated from CH_4 is the activation of oxidant. The most desired product of CH_4 transformation is methanol, which is a significant and valuable commodity in the chemical industry.

The selective oxidation of CH_4 to methanol over metallozeolites was suggested to be a promising way of CH_4 utilization. Thus, the four mechanisms for C-H bond activation in CH_4 were proposed in the literature: oxidative addition, electrophilic activation, sigma-bond metathesis, and the reactive metal-oxygen (O) species.[10] The reactive O-species strategy is employed by nature and metallozeolites to activate strong C-H bonds. The formation of isolated, highly reactive oxygen species is a result of the activation of an oxidant over TMIs in zeolites. Subsequently, various oxidants may be employed (e.g., N_2O, NO, H_2O_2, O_3, H_2O) for CH_4 oxidation. However, these oxidants cannot be compared with the free and available atmospheric molecular oxygen.

1.3 Selective oxidation of methane over TMI-containing zeolites

Over recent years, the use of zeolites containing TMIs have been proposed as a chemical looping approach for selective CH_4 oxidation to methanol. In this process, CH_4 is oxidized by O_2/N_2O, which are previously activated over TMI-containing zeolites. However, in comparison to N_2O, molecular oxygen, due to its easy availability and eco-friendly properties, represents the most desirable oxidant from both environmental and economic points of view. Methanol produced from CH_4 has the dual potential acting both as an energy carrier and as a key chemical raw material for obtaining oxygenates.

The majority of current research focusing on CH_4 oxidation over metallozeolites is directed toward the behavior of Fe and Cu cations embedded in various zeolite

topologies: ZSM-5, MAZ, MFI, MOR, FER, *BEA, FAU, or ZSM-13.[11, 12] Since the first report by Panov et al.[13] in 1990 on the formation of highly reactive oxygen species (α-oxygen, α-O) upon CH_4 oxidation with N_2O over Fe-ZSM-5 (stabilization of the Fe(II)/α-O sites), numerous investigations have been conducted.[11, 12] Moreover, Co, Ni, and Mn-based zeolites have also been used as catalysts for selective CH_4 oxidation.[11]

1.3.1 Activation of N_2O over TMI-modified zeolites

Panov et al.[13] reported that previously activated at 900°C Fe-ZSM-5 efficiently decomposed N_2O at temperatures ≤ 300°C. As a result of this interaction, the highly reactive α-O presented as $(FeO)^+$ bound to the zeolite surface is formed. Moreover, it was shown that only a small fraction of the present Fe species in the studied Fe-ZSM-5 is catalytically active in N_2O activation. The oxidation properties of α-O were confirmed in the CH_4 to CH_3OH transformation.

Jisa et al.[14] experimentally confirmed the structure of α-O from N_2O splitting over Fe-FER, Fe-MFI, and Fe-BEA zeolites. Their multi-spectroscopic results and DFT calculations have shown the structural models where two cooperating Fe(II) cations located in two adjacent β cationic sites of FER form the active site responsible for the N_2O decomposition and stabilization of α-O.

The next experimental study of the α-O formation and CH_4 oxidation has been made by Snyder et al.[15] and Bols et al.[16] for Fe-BEA* and Fe-SSZ-13 matrices, respectively (Fig. 2). Snyder et al. have reported that Fe active centers performing α-O from N_2O are a mononuclear, high-spin with the square planar Fe(II) coordination environment. Further, DFT studies suggest that Fe(II) exhibits a square planar environment residing within a β-6MR with two Al atoms.

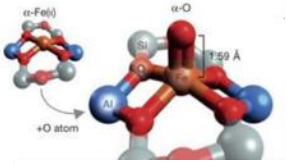

Fig. 2. The structure of the α-O in the zeolite *BEA. Copyright 2016 Nature Publ. Group[16].

Another zeolite catalyst for N_2O dissociation and subsequent CH_4 to methanol oxidation represents the materials containing Cu species.[17] Catalytic processes based on Cu-zeolite catalysts present several challenges. These include the need for high-low temperature cycles, the necessity of water or water-organic medium extraction of methoxy groups strongly bound to the catalyst, the low yields in the catalytic regime, and the main disadvantage is catalyst destruction.

Besides, Co-containing zeolites with the topology of MFI, MOR, BEA, ZSM-11 and Y exhibited excellent catalytic performances in N_2O decomposition.[18] Catalytic study results of N_2O decomposition confirmed that Co-ZSM-5, together with Co-BEA and Co-ZSM-11, are the most active structures. In contrast, the Co introduced to Y zeolite exhibits very low catalytic activity in N_2O abatement reactions. In the literature, there is limited information about the behavior of Ni- and Mn-containing zeolites in the N_2O decomposition.

1.3.2 Activation of O_2 over TMI-containing zeolites

The most extensive studies of O_2 activation and subsequent CH_4 to methanol oxidation were performed over Cu-zeolites.[19] It was assumed that the difference in activity may be associated with the nature of active sites present in Cu-exchanged zeolites of various structural types. The products of CH_4 oxidation over Cu-zeolites are attached to the zeolite surface, and to remove them, the use of effluent is needed. Also, the presence of Ni in zeolites leads to activation of O_2 and selective oxidation of CH_4. Particularly, Ni-ZSM-5 activated in O_2 flow selectively oxidized CH_4 to methanol already at 150°C. Moreover, also for Ni-ZSM-5, the oxidation products required product extraction into the liquid products from the catalyst. DFT results suggested that $[Ni_2(\mu O)]^{2+}$ center is the active site for CH_4 oxidation.[20]

The other class of catalysts represents the Co-exchanged zeolites. Beznis et al.[21] have shown that Co-ZSM-5 zeolite can be used as a catalyst for CH_4 oxidation by O_2 at low temperatures. Significantly, by employing distinct preparation techniques, it is possible to modulate the catalytic activity and selectivity of the catalytic system. Thus, in the Co-ZSM-5 prepared by ion exchange at RT, the majority of Co was found to be in ion exchange positions. This sample exhibited the highest selectivity toward formaldehyde formation. In contrast, impregnated Co-ZSM-5, which contain primarily cobalt oxide species (CoO and Co_3O_4), showed greater selectivity toward CH_3OH formation.

1.4 O_2 activation over binuclear cationic centers in FER zeolites

Recently, Tabor et al.[22] reported a new feature of Fe-zeolites that reveals the cooperation of two Fe(II) centers in O_2 activation. Moreover, the stabilized oxygen species (α-O) formed after O_2 splitting selectively oxidized CH_4 to methanol at RT. The binuclear Fe(II) species (Fig.3A), in contrast to the isolated Fe(II) ions in zeolites, take part in the four-electron reactions process resulting in O_2 splitting. The Fe(II) binuclear centers are constituted by two Fe(II) cations located in β cationic position with two Al atoms in 6-MR of FER distant at ca. 7.5 Å. The previous study focused on the analysis of the Al atoms organization in FER (Si/Al 8.6) and demonstrated that the concentration of Al pairs in the β-site is high (50% of the total Al atoms), indicating that approximately 94% of the 6-MRs of the β-site can accommodate bare divalent cations.[23] Therefore, at least 88% of the β sites are capable of forming binuclear Fe(II) structures. Conversely, the investigation demonstrated that the concentration of Al pairs in the α site is relatively low (10% of all the Al atoms), indicating that only a minimal proportion of the α sites can form binuclear Fe(II) structures.

The DFT calculations and spectroscopic studies have confirmed the ability of the binuclear Fe(II) sites in the FER matrix (Fig. 3) to split O_2. The binuclear Fe(II) structures cleaved the O=O double bond and formed a pair of the α-O atoms on the two Fe(II) cations (Fig. 3C). Furthermore, the splitting of O_2 over binuclear Fe(II) centers in FER and formation of α-O was confirmed by in-situ FTIR and Mössbauer studies already at RT. Both methods provide a spectroscopic fingerprint of α-O, which is clearly visible in FTIR spectra as the newly formed band at 890 cm^{-1} after O_2 treatment and in the Mössbauer study as parameters isomer shift (IS) = 0.29 and quadrupole splitting

(QS) = 0.78. Additionally, FTIR spectroscopy confirmed the stability of the previously formed α-O up to 200°C.

In order to check the oxidation properties of α-O stabilized on Fe(II) after O_2 splitting, CH_4 was used as a probe molecule. The mass spectrometry results confirmed the formation of methanol with a significantly higher yield of methanol (75 $\mu mol/g_{cat}$) in comparison to the previously reported data over TMI-zeolites. It should be noted that water or an organic solvent is not needed here to extract the oxidation products from the zeolite surface.

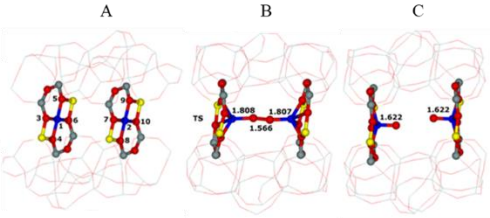

Fig. 3. Model of O_2 splitting over Fe (II) binuclear centers in FER after molecular dynamics (MD) simulations. (A) Fe(II) binuclear center, (B) [Fe-O-O-Fe] transition state (TS), and (C) [Fe=O O=Fe] product. The distances are in Å. Si atoms are in gray, O atoms are in red, Al atoms are in yellow, and Fe atoms are in blue.

II Aims of the work

This dissertation thesis discusses the determination of the possibility of the formation of distant binuclear structures in zeolite matrices and their reactivity toward small molecules activation.

The following questions were posed:

1. How to analyze the O_2 activation and following CH_4 oxidation over Fe-FER using spectroscopic techniques?
2. Do TMI ions other than Fe(II) ions form binuclear centers in FER for O_2/N_2O cleavage?
3. Could zeolites of topologies other than FER stabilize Fe(II) binuclear active centers for O_2 splitting?
4. Does the α-O originating from N_2O and O_2 splitting stabilized on the binuclear centers of Co(II), Ni(II), Fe(II) and Mn(II) in FER zeolites react with CH_4 at low temperatures?
5. How is the cation speciation in FER and MOR zeolites reflected in the catalytic performance of Fe-zeolites in the CR_{N2O} and SCR_{N2O} of N_2O by CH_4?

To address these queries, the subsequent steps were realized:

1. Developing a methodology based on the spectroscopic methods for analyzing α-O formation over Fe-FER.
2. Potential to form binuclear centers of Co(II), Ni(II), and Mn(II) in FER, their speciation, and the effect of metal loading using FTIR spectroscopy.

3. Study of the possibility of forming binuclear centers in MOR, *BEA, and LTA zeolites, including determining Al distribution in MOR zeolite.
4. Monitoring of the process of N_2O/O_2 splitting toward α-O formation and its stabilization on Co(II), Ni(II), Fe(II), or Mn(II) in FER for the following CH_4 oxidation.
5. Realization of the catalytic tests over Fe-FER and Fe-MOR under conditions of CR_{N2O} and SCR_{N2O} of N_2O reduction by CH_4.

III Results and discussion

Spectroscopic studies of α-O formation by the dissociation of O_2 and N_2O over metallozeolites were performed, and the reactivity of α-O toward CH_4 oxidation was investigated. As catalysts for O_2 and N_2O activation, the following zeolite topologies were used: FER containing Co(II), Ni(II), Mn(II), or Fe(II) cations, and Fe(II)-MOR. The catalytic activity of α-O was tested in a CH_4 to methanol transformation. The experimental data obtained from the activation of O_2/N_2O over metal-containing FERs (Co(II), Ni(II), Mn(II), Fe(II)), and Fe(II)-MOR were supported by a theoretical study, which included computational modeling, electronic structure calculations, molecular dynamics, and geometry optimizations. A theoretical study was also extended to Fe(II)-*BEA and Fe(II)-LTA zeolites.

3.1 How to analyze the O_2 activation and following CH_4 oxidation over Fe-FER using spectroscopic techniques?

The study of the formation, stabilization, and evolution of α-O from O_2 and N_2O dissociation over metallozeolites, as presented in this thesis, was possible thanks to the careful choice of a combination of several characterization techniques. The best method for the detection of the binuclear center's ability to split O_2/N_2O to result in α-O formation is the reaction test with CH_4. The main feature of α-O is its high oxidation potential to transform CH_4 into methanol. Previously, the formation of α-O from O_2 over Fe binuclear centers in FER had been confirmed at RT under ex-situ conditions.[22] The studied Fe-FER had to be activated after the redox cycle (O_2/CH_4) in order to perform the splitting of the O_2 and the CH_4 oxidation. Thus, to extend the application of Fe-FER as a catalyst for CH_4 oxidation by O_2, we focused on performing the study at an elevated temperature under isothermal conditions so as to exclude the catalyst activation step after the redox cycle (O_2/CH_4). To analyze the oxidation properties of the α-O formed by O_2 splitting, we used a combination of in-situ XANES, Mössbauer, FTIR, and mass spectrometry to monitor its interaction with the CH_4. Most of the measurements and examinations of the α-O formation were conducted at 220°C, and this temperature is based on previous results concerning the thermal stability and optimal conditions for O_2 splitting over Fe-FER.[22]

Mössbauer spectroscopy was used to analyze the oxidation state and the coordination of the Fe species in the ^{57}Fe-FER (Fe/Al 0.04) sample, which was prepared intentionally for this study. The Mössbauer spectrum of the evacuated ^{57}Fe-FER (Fig. 4a) was deconvoluted into three components (D1–D3), the isomer shift (IS) value confirming the exclusive presence of divalent Fe species laced in β sites (D1–D2) and α site (D3).[22] The analysis of the Mössbauer spectrum of ^{57}Fe-FER, recorded after O_2 interaction

confirmed the splitting of O_2 over the Fe(II) centers located in the β cationic position and the stabilization of the active O_2 form ($[Fe(IV)=O]^{2+}$). Deconvoluted Mössbauer spectrum of Fe-FER recorded after O_2/CH_4 interaction confirmed the presence of exclusively Fe(II) species. This observation clearly indicates that the previously formed α-O species was again reduced after CH_4 treatment to Fe(II).[16]

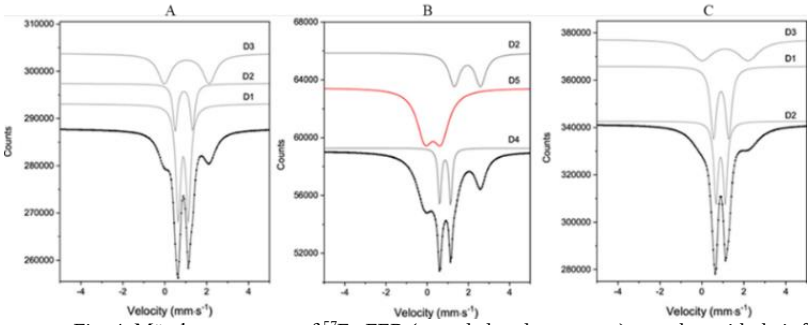

Fig. 4. Mössbauer spectra of ^{57}Fe-FER (recorded under vacuum), together with their fits, collected after the following treatments: (A) 3h evacuation at 450°C under dynamic vacuum; (B) interaction with O_2 for 40 min at 220°C; and (C) interaction with CH_4 for 30 min at 220°C.

Similarly to the Mössbauer study, an analysis by time-resolved in-situ XANES spectroscopy under the O_2/CH_4 treatment of Fe-FER was performed. Fig. 5 depicts the XANES spectra of Fe-FER (Fe/Al 0.04) collected after activation of the sample in He flow at 450°C (in beige), after O_2 oxidation (in green), and following the interaction with CH_4 (in pink). The XANES spectrum of FeO (Fig. 5 in red) was used to confirm the presence of Fe(II), and the spectra of Fe_2O_3 (Fig. 5 in black) and NO/O_2 (Fig.5 in blue) were used as a reference for the Fe(III). Importantly, the XANES spectrum recorded after evacuation of the Fe-FER (Fig. 5 in beige) indicated that a major fraction of the Fe species in the Fe-FER was present as Fe(II), as reflected by a shift in the absorption edge toward lower energies. The shoulder arising at the absorption edge at ca. 7120 eV, forming due to a 1s→4p transition, confirmed the square planar symmetry of the Fe(II), typical for Fe(II) in β cationic positions. The interaction of Fe-FER with O_2 (Fig. 5 in green) resulted in the oxidation of the Fe(II) species present in the activated Fe-FER to Fe(III). Moreover, the absorption edge after O_2 treatment was shifted to higher energies, and a pre-edge feature occurring at approximately 7114.4 eV increased this, indicating the formation of a five-fold coordination of the Fe ion.

The XANES spectrum of previously O_2-oxidized Fe-FER treated by CH_4 is presented in Fig. 5 (in pink). The interaction of the CH_4 with the O_2-oxidized sample led to the reduction of all the Fe(III) to Fe(II), as can be seen in Fig. 5 (in pink) by the shifting of the spectrum to the position typical for Fe(II), as observed in the activated sample (Fig. 5 in beige). The XANES spectra recorded under NO/O_2 (Fig. 5 in blue) showed a deeper oxidation of the Fe species compared to the O_2, which suggests that some Fe species were resistant to oxidation by O_2 and a stronger oxidizing agent may be required.

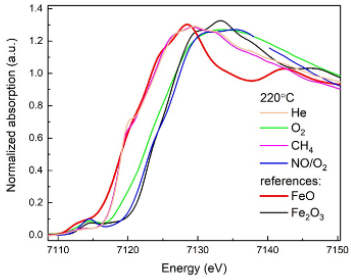

Fig. 5. XANES spectra of Fe-FER recorded under He activation at 450°C (in beige), O_2 at 220°C (in green), and CH_4 at 220°C (in pink) treatments. For reference, FeO (in red), Fe_2O_3 (in black), and NO/O_2 (in blue).

In-situ FTIR spectroscopy was used as the third method in developing the complex methodology for monitoring α-O over Fe-FER. To illustrate this approach, the in-situ FTIR spectra (Fig. 6) of the Fe-FER activated at 450°C (in red) are presented after interaction with O_2 (in blue) and CH_4 (in green).

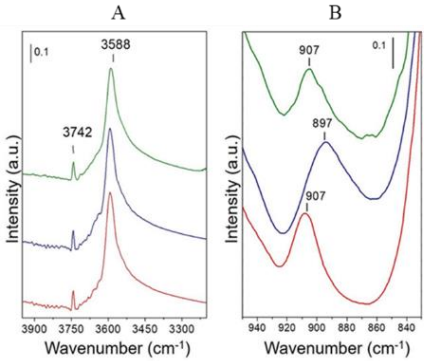

Fig. 6. FTIR spectra of Fe-FER in the range of: (A) OH; and (B) T–O–T. Activation over 3 h at 450°C in He (in red), 1 h of O_2 interaction at 220°C (in blue), and CH_4 treatment at 220°C (in green).

The spectra were analyzed in the region of the OH (Fig. 6A) and T–O–T (Fig. 6B) vibrations. The positions of the silanol groups (3742 cm^{-1}) and Brønsted acid sites (Si-OH-Al) (3588 cm^{-1}) observed in the evacuated samples did not change in either the O_2 or CH_4 treatment. This indicates that the OH groups of the Fe-FER did not participate in the O_2/CH_4 redox cycle. The presence of a band at 907 cm^{-1} (Fig. 6B) confirmed the location of Fe(II) in the β cationic position of the FER structure. Interaction with O_2 led to the formation of a new band at 897 cm^{-1}. Based on data from the literature, this was identified as a spectral fingerprint of α-O ($[Fe(IV)=O]^{2+}$).[13, 22]

To investigate the oxidation properties of $[Fe(IV)=O]^{2+}$, the FTIR spectrum was recorded after CH_4 treatment at 220°C. Following the interaction of CH_4 with the O_2-pre-

oxidized Fe-FER, the intensity of the band at 897 cm^{-1} decreased significantly, and the band at 907 cm^{-1}, which is characteristic of Fe(II) in β sites, reappeared.[25] These results show, for the first time, that cooperating Fe(II) species are also effective in α-O formation from O_2 at elevated temperatures. Moreover, this indicates that the possible reaction products do not interact with the acid centers of the zeolite. The results presented above confirm the formation of the α-O over Fe-FER, but they do not describe the kinetics of its formation, which is a crucial point in catalytic studies. For this purpose, FTIR spectroscopy was applied to monitor the behavior of the Fe sites interacting with O_2 under in-situ conditions at 220°C. Analysis of the FTIR spectra (Fig. 7A) in the region of the T–O–T vibrations showed that, within an interaction time of 0-60 min, the intensity of the band at 907 cm^{-1}, assigned to Fe(II) in the β cationic position, decreased with the increasing intensity of the band characteristic for the α-O at 897 cm^{-1} (Fig. 7B).[22] This correlation between the decreasing concentration of β sites (band at 907 cm^{-1}), estimated from the FTIR spectra, and the formation of the band at 897 cm^{-1} is depicted in Fig. 7A. It was confirmed by an in-situ FTIR study that, to oxidize all the Fe(II) in the β sites and to reach the highest intensity of the band typical for α-O, a time of 60 min was required.

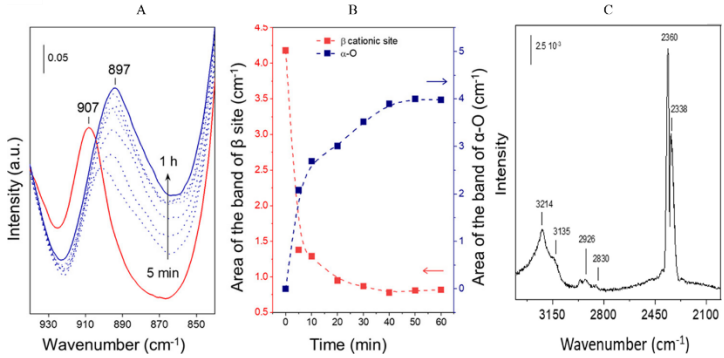

Fig. 7. (A) FTIR spectra of the kinetics of α-O formation over Fe-FER at 220°C; and (B) temperature dependence of the evolution of the bands characteristic for α-O and Fe(II) in β sites. (C) FTIR spectra of the gas phase acquired during the reaction of the Fe-FER with O_2 and CH_4.

In the next step, the thermal stability of the α-O over Fe-FER was investigated using FTIR spectroscopy under in-situ conditions. The α-O previously formed at 220°C after the interaction of Fe-FER with O_2 was monitored every 20°C up to 380°C. The intensity of the band at 897 cm^{-1}, assigned to the α-O, remained the same up to 260°C, above which the band intensity decreased in a stepwise manner. These findings indicate that the α-O was stable up to 260°C but decomposed above this temperature, presumably via the recombination of two α-O.[22]

To determine the oxidation products, an FTIR analysis of the gaseous products of the interaction of the α-O stabilized on the Fe-FER with CH_4 at 220°C was performed (Fig. 7C). The presence of bands with low intensity at 2926 and 2830 cm^{-1}, characteristic of the vibrations of methoxy species, indicated methanol formation.[24, 26] The bands at 2360 and 2338 cm^{-1} corresponded to carbon dioxide (CO_2) stretching vibrations. The appearance of CO_2 among the reaction products, together with the presence of a band in

the region of the OH vibrations at 3214 cm^{-1}, typical for OH vibrations in H_2O, suggest the overoxidation of CH_4 and/or the products initially formed during CH_4 oxidation.

Mass spectrometry was used as an additional method to analyze the products of CH_4 oxidation by the α-O previously formed on the Fe(II) species in the FER by O_2 splitting at 220°C. The Fe-FER sample was activated at 450°C, cooled down to 220°C, and at this temperature, oxidized by O_2 and subsequently interacted with CH_4. Three consecutive cycles of the interaction of the Fe-FER with O_2 and CH_4 were performed. The mass spectrum exhibited signals with m/z = 31 (methanol) and m/z = 44 (CO_2). The methanol productivity obtained at 220°C varied over the three subsequent redox cycles between 0.20 and 0.38 $\mu mol/g_{cat}$. The obtained results reveal that the oxidation products of CH_4 formed by O_2 were detected in the gas stream, which proves their spontaneous release at 220°C from the active Fe sites and from the zeolite channel system to the gas phase without the need for effluent usage. The FTIR and mass spectrometry results confirmed the formation of the same products of CH_4 oxidation by the α-O stabilized on the Fe-FER.

The spectroscopic results from the in-situ Mössbauer, XANES, and FTIR spectroscopy confirmed that the characterization methodology developed for monitoring the O_2 interaction over the Fe-FER can be successfully used for analysis of the formation, kinetics, and oxidation properties of α-O. By including the results from the mass spectrometry and FTIR analysis in the gas phase, it was also possible to detect the oxidation products. The results indicate that two Fe(II) centers with planar geometry embedded in the FER worked together in the redox cycle. When the Fe-FER interacts with O_2, $[Fe(IV)=O]^{2+}$ is produced, which is then reduced by CH_4 to the Fe(II) centers. It was found that the α-O formed under throughflow conditions was stable up to 260°C and exhibited oxidation properties in CH_4 to methanol oxidation. Methanol production was recorded in the gas phase through the use of FTIR and mass spectrometry. Combining the methodologies of in-situ Mössbauer, XANES, and FTIR spectroscopy, mass spectrometry, and FTIR analysis in the gas phase can be used as a tool for the determination of potential TMI-containing zeolites for O_2 activation and CH_4 oxidation.

3.2 Do TMI ions other than Fe(II) ions form binuclear centers in FER for O_2/N_2O cleavage?

In this section, special attention is given to the analysis of the siting and location of bare divalent cations of Co(II), Ni(II), and Mn(II) in the extra-framework cationic sites in the FER matrix (Si/Al 8.6, M/Al 0.04 – 0.33). The introduction of cations of Co, Ni, or Mn to the FER was performed by ion exchange or impregnation methods. The ion exchange method was used to prepare a whole concentration range of Co-FER (Co/Al 0.04 – 0.33) zeolites and low-loaded samples with Ni and Mn/Al (0.04 – 0.16 M/Al). For the Ni- and Mn-FER samples (0.16 – 0.38 M/Al), it was necessary to use the impregnation method. These two preparation methods were used because of difficulties associated with the preparation of high-loaded samples in the ion exchange procedure. The study required samples with high TMI loading, as this guarantees the formation of high-fraction catalytically active binuclear centers in the zeolite framework. The sizes of the metal atom radii, types of precursors, prepa6ration conditions, pH of the solution, the concentration of TMIs, temperature, and contact time between the zeolite and the precursor were all

considered to be the most probable factors influencing the introduction of cations into the FER structure.

Analysis of the FTIR spectra of the Co-, Ni-, and Mn-FER with M/Al 0.16 in the region of the T–O–T vibrations revealed the presence of M(II) bare cations in α, β, and γ cationic positions.[24] In all the studied samples, the majority (70% – 75 %) of M(II) cations were located in β positions, which is regarded as a precondition for the formation of binuclear centers. The rest of the M(II) cations were in the α (15% – 20 %) and γ (10%) sites. In more concentrated samples (M-FERs with M/Al > 0.16 up to a limit of M/Al 0.33), the occupation of cationic positions by bare cations depended on the specific cation and was approximately as follows: Mn(II) – 80%, Ni(II) – 55%, and Co(II) – 98%. As also shown, the share of occupation of the α and β positions strongly depended on the individual cations.[25]

In general, all the prepared Co-, Ni-, and Mn-FER samples were close to the maximum loading of bare divalent cations (M/Al 0.33). Analysis of the obtained data indicated that, for the M-FER samples with M/Al > 0.22, at least 50% of the M(II) cations were located in β cationic positions that could form the binuclear centers that can perform O_2/N_2O activation. The results showed that the TMIs (Co, Ni, and Mn) had been introduced and had stabilized as M(II) species over the FER topology, as confirmed by FTIR spectroscopy of the region of the perturbed T–O–T vibrations. These M-FERs with high loadings of bare M(II) in cationic sites were successfully prepared, and a unique type of active site – binuclear structure was formed.

3.3 Could zeolites of topologies other than FER stabilize Fe(II) binuclear active centers for O_2 splitting?

The DFT method was used to understand the role of zeolitic matrices for the stabilization of Fe sites forming binuclear centers in FERs that are active in O_2 splitting. The DFT calculations were used to analyze the possibility of O_2 splitting over Fe(II) embedded in MOR, *BEA and LTA zeolites. In this study, we focused on evaluating the potential of zeolites with topologies other than that of FER to find an arrangement suitable for the formation of an optimal distance between two Fe(II) ions so it could cooperate in O_2 dissociation. For this purpose, ^{27}Al MAS-NMR and UV-Vis spectroscopy were employed to determine the organization of Al atoms in MOR zeolites used as catalysts for CR_{N2O} and SCR_{N2O} reactions (Section 3.5).

As previously established, the formation of binuclear Fe(II) centers in FER with the potential for splitting O_2 is controlled by certain structural and geometrical requirements, including: i) the presence of Al atoms in pairs that stabilize the Fe(II) ions, ii) a parallel arrangement of the two zeolite rings containing the Fe(II) cations; and iii) an optimal distance between two Fe ions of about 7 – 9 Å.[22]

Accordingly, the DFT calculations were employed to interrogate the structural properties of MOR, *BEA, and LTA zeolites in fulfillment of these structural demands (i.e., having Fe(II) in their binuclear centers and their potential for splitting O_2). The results of the DFT calculations suggested that the binuclear Fe(II) sites with suitable parameters could be accommodated in topologies other than the FER topology, that is, in MOR, *BEA, and LTA zeolites. The calculations showed that the potential for the splitting of O_2 over Fe-zeolites strongly depended not only on cation distance but also on

their mutual orientation. It has been found that the axial arrangement of the Fe centers in MOR and *BEA zeolites enabled the splitting of O_2 and the formation of α-O. Conversely, the non-parallel orientation of Fe binuclear centers in the LTA zeolite precludes O_2 activation. The results of this study have revealed that the ability for O_2 cleavage represents a general property of distant binuclear Fe(II) centers optimally stabilized in zeolites, thus suggesting the possibility of developing various Fe zeolite-based systems for O_2 activation for direct hydrocarbon oxidations

Moreover, the nature of Fe active centers in MOR responsible for the CR_{N2O} and SCR_{N2O} reactions was analyzed. As previously shown, the organization of Al atoms in the zeolite matrix plays a crucial role in the stabilization of the Fe active sites.[5] Thus, a study was based on a determination of the distribution of the Al atoms in the commercially available MOR (Si/Al 9.2). The Al atom organization in the MOR zeolite was investigated using a combination of ^{27}Al MAS-NMR and UV-Vis spectroscopy and the methodology described previously.[5] The ^{27}Al MAS-NMR spectrum of hydrated MOR confirmed that the Al atoms were exclusively located in the framework positions of the MOR. The determination of the distribution of Al atoms in the MOR matrix was based on the application of Co(II) ions as probes monitored by UV-Vis spectroscopy supported by quantitative data from chemical analysis. The results obtained from the UV-Vis and XRF methods showed that the MOR matrix contained the majority (72%) of the Al atoms forming Al pairs. This type of Al distribution is crucial for stabilizing divalent cations. The rest (28%) of the Al atoms in the MOR zeolite were present as single Al atoms.

3.4 Does the α-O originating from N_2O and O_2 splitting stabilized on the binuclear centers of Co(II), Ni(II), Fe(II) and Mn(II) in FER zeolites react with CH_4 at low temperatures?

3.4.1 O_2 splitting and subsequent CH_4 interaction at low temperature

Herein, the investigations of the dissociation of O_2 over binuclear centers formed by Ni(II), Co(II), and Mn(II) in FER will be discussed. The interaction of O_2 with Ni(II)-, Co(II)-, and Mn(II)-FER at RT was monitored by in-situ FTIR spectroscopy. The analysis of the FTIR spectra of the M-FERs (where M = Ni, Co or Mn) in the T–O–T vibration region revealed that, for all the studied zeolites, after exposure to O_2, the band in the region[25] attributed to the accommodation of bare M(II) cations located in the β cationic position disappeared, while a new band is formed at around 870 cm^{-1}. This new band remained stable after the gas-phase O_2 had desorbed at RT. As previously indicated, the vanishing of the band at about 920 cm^{-1}, characteristic of bare M(II) cations accommodated in the β site in M(II)-FERs, and the simultaneous formation of the new band at lower frequencies (870 cm^{-1}) due to stronger perturbation in the zeolite ring, indicates that the M(II) was oxidized by the O_2 to $[M(IV)=O]^{2+}$. The band at around 870 cm^{-1} was established as an FTIR characteristic of the α-O.[22] These results indicated that, over all three FER samples, the O_2 molecule was cleaved over the distant binuclear Ni(II), Co(II), and Mn(II) centers present in the FERs, and a pair of distant α-O atoms were formed, (i.e., analogous to the Fe-FER).[22] These findings are the first evidence of the splitting of O_2 and the formation of the α-O on binuclear sites other than in Fe-FER.[22]

All three M(II)-FER samples, featuring pairs of the distant α-O atoms originating from the O_2 cleavage, subsequently interacted with CH_4. This interaction led to the disappearance of the band at 870 cm^{-1} and the appearance of the band at 920 cm^{-1}, corresponding to the bare M(II) cations accommodated in the β cationic sites. The regeneration of the band at 920 cm^{-1} indicates that the CH_4 interacted with the $[M(IV)=O]^{2+}$ (formed after O_2 treatment) to form volatile products.

To detect the volatile products of CH_4 oxidation by $[M(IV)=O]^{2+}$, mass spectrometry was applied. The M(II)-FER samples were oxidized by O_2 and subsequently interacted with CH_4 at RT, respectively. The mass spectrum revealed the presence of a signal with m/z = 31 that confirmed the formation of methanol in the gas phase. These results proved that the α-O atoms from the O_2 splitting over all the studied M(II)-FER samples could directly oxidize CH_4 to methanol. The yields of methanol produced per gram of zeolite were 20 $\mu mol/g_{cat}$ for Co-FER, 42 $\mu mol/g_{cat}$ for Mn-FER, and 116 $\mu mol/g_{cat}$ for Ni-FER per cycle. These methanol yields indicate that the Ni-FER had the best performance in the direct oxidation of CH_4 to methanol. Because the methanol was detected in the gas stream, it can obviously be released from the active sites and zeolite channel system to the gas stream without the need for effluent.

3.4.2 N_2O decomposition and subsequent CH_4 treatment at low temperature

In order to assess the redox behavior of binuclear Co, Ni, and Fe in FERs, the interaction of N_2O and CH_4 was analyzed by FTIR spectroscopy and mass spectrometry. The FTIR results from the interaction of N_2O with the M-FERs (where M = Co(II), Ni(II) or Fe(II)) at RT clearly showed that the bands of the M(II) cations located in the β cationic positions disappeared, while the two new bands are formed at approximately 950 and 880 cm^{-1}. The band at 880 cm^{-1} was attributed to the $[M(IV)=O]^{2+}$ complex, featuring the α-O, similarly to in the Fe-FER. The weak band at 950 cm^{-1} was assigned to the ligand complex M(II) with N_2O. The oxidation properties of the α-O formed on the Co-, Ni-, and Fe-FER samples were investigated through the selective oxidation of CH_4, monitored by in-situ FTIR spectroscopy. The FTIR spectra of the M-FERs recorded after interaction of the previously N_2O-oxidized M-FER with CH_4 indicated that the band at 880 cm^{-1}, which corresponded to the α-O, had disappeared completely, while the band at around 920 cm^{-1}, characterizing the bare M(II) cations accommodated in the β site, had reappeared. The emergence of the band at about 920 cm^{-1}, which characterized the bare divalent cations located in the β site, suggests the protonation of methoxy groups.

Analysis of the FTIR spectra in the region of the C-H stretching vibrations (3000 – 2830 cm^{-1}) revealed the presence of a band at 2960 cm^{-1} corresponding to formate species bound to the Fe cation, a band at 2853 cm^{-1} attributed to CH_3OH, and a band at 2920 cm^{-1}, which was assigned to the methoxy group bound to the Fe cation.[26] The bands in the region of methyl group (δCH_3), carboxyl group (δCOH), and νCO vibrations (1800 – 1290 cm^{-1}) appeared at 1666 and 1355 cm^{-1} and were assigned to formate anions bound to the Fe cation, and at 1642 cm^{-1}, attributed to formaldehyde adsorbed on the Fe cation.[26] The presence of bands characterizing methanol, formaldehyde, and formate suggests the protonation of methoxy groups in the M(II)-FERs with binuclear M(II) species. The higher protonation activity of all three M-FERs resulted in the creation of protonated oxidation products that is, methanol, formaldehyde, and formic acid.

The oxidation products of CH_4 over N_2O-oxidized M-FERs (M = Co, Ni, or Fe) were also monitored using mass spectrometry in order to confirm the protonation of the methoxy groups and to determine the composition of the oxidation products. The previously N_2O-oxidized M-FERs have interacted with CH_4, and the products of the oxidation were detected by mass spectrometry. The mass spectrometry results confirmed the formation of methanol (m/z = 31) and small amounts of other oxidation products, such as formaldehyde, formic acid, dimethyl ether, and CO_2. The yields of methanol produced per gram of zeolite were 200 μmol/g_{cat} for Co-FER, 290 μmol/g_{cat} for Ni-FER, and 32 μmol/g_{cat} for Fe-FER per cycle. These results confirm that the active sites for the formation of the α-O and CH_4 oxidation involved two cooperating M(II) cations.

3.5 How is the cation speciation in FER and MOR zeolites reflected in the catalytic performance of Fe-zeolites in the CR_{N2O} and SCR_{N2O} of N_2O by CH_4?

3.5.1 Detections of Fe(II) in studied Fe-zeolites

In order to analyze the influence of zeolite topology on the catalytic performance in CR_{N2O} and SCR_{N2O} reactions, Fe-FER and Fe-MOR with similar Fe loadings were used. The Fe was introduced to both the FER (Si/Al 8.6) and MOR (Si/Al 9.2) matrices via impregnation in acetylacetone. To determine the role of various Fe species in the CR_{N2O} and SCR_{N2O} processes, we intentionally prepared the samples to contain low (below 0.8 wt.%) and high (above 1.5 wt.%) Fe loadings that differed in the type of Fe sites The studied samples were marked Fe-FER-32, Fe-FER-70, Fe-MOR-23, and Fe-MOR-95, where the number represented the $3Fe^{3+}$/Al ratio.

Carbon monoxide (CO) and NO were used as probe molecules for the detection of Fe(II) in the samples Fe-FER-32, Fe-FER-70, Fe-MOR-23, and Fe-MOR-95. The analysis of the FTIR spectra after CO adsorption verified that a band at 2200 cm^{-1}, typical for Fe(II)-CO, was formed in all the samples.[27] This confirmed the presence of the Fe(II) species in all the studied Fe-zeolites. In the Fe-MOR samples, the intensity of the Fe(II)-CO bands significantly increased with increasing Fe loading, indicating that, in the MOR matrix, the specific cationic positions accessible to Fe(II) were gradually populated at increasing Fe concentrations.

The NO adsorption was used to better evaluate the speciation of Fe(II) due to the strong NO affinity toward Fe(II), which results in the formation of stable nitrosyl species.[28] In the studied Fe-FERs, only one type of Fe(II)-NO species was revealed at around 1820 cm^{-1}, as indicated by the symmetrical shape of the corresponding band. This indicates that the active Fe(II) species capable of adsorbing only one NO molecule was introduced into the FER matrix at low Fe loading, while the active Fe(II) species adsorbing two or three NO molecules were introduced at higher Fe loading. In the NO adsorption over the Fe-MOR samples, the nitrosyl region showed an intense band at 1880 cm^{-1} with a shoulder at about 1910 cm^{-1}, indicating two types of Fe(II)-NO mono nitrosyl species. A weak band at 1760 cm^{-1} was ascribed to Fe-$(NO)_2$ dinitrosyls, and bands at 1820 and 1925 cm^{-1} were typical for Fe-$(NO)_3$ trinitrosyl species. Based on this, at least three types of Fe(II) species were inferred in different positions of MOR cavities – two species able to adsorb a maximum of one molecule of NO, and a third species filling its coordination sphere with two or three NO molecules.

3.5.2 Role of zeolite topology in CR_{N2O} and SCR_{N2O} reactions over Fe-FER and Fe-MOR: Catalytic and operando study

All the studied Fe-FER and Fe-MOR catalysts were highly active in the reduction of N_2O by CH_4 (CR_{N2O}). Under laboratory conditions, the N_2O conversion reached 100% in the range 350 – 400°C, during which the CH_4 conversion reached its maximum value (about 30%), remaining constant at higher temperatures. With increasing Fe content in the zeolite, the activity increased nearly proportionally over the Fe-FER catalysts but was less over the Fe-MOR catalysts.

When excess O_2 was added to the N_2O+CH_4 mixture (SCR_{N2O}), both the Fe-MOR and Fe-FER systems were still highly active for N_2O reduction with CH_4. Again, by increasing the Fe loading, the N_2O conversion increased over the Fe-FER catalysts but was less over the Fe-MOR catalysts.

A comparison between the catalytic activity of the Fe-MOR and Fe-FER catalysts showed that N_2O abatement under conditions of CR_{N2O} action only negligibly depended on the zeolite matrix used, suggesting the presence of similar amounts of Fe(II) working sites in both zeolites at similar Fe loading. Contrastingly, the N_2O abatement in the SCR_{N2O} process was higher on the Fe-FER than on the Fe-MOR catalyst.

Operando FTIR experiments were performed to obtain information on the pathways of the CR_{N2O} and SCR_{N2O} and the key intermediates stabilized on the active Fe centers are involved in these processes. It should be stressed that, regardless of the concentration of the Fe in the studied MOR or FER, the general trend in the interaction with the CR_{N2O} and SCR_{N2O} detected under operando conditions was the same. The spectra of the Fe-MOR-23 and Fe-FER-32 catalysts under a N_2O+CH_4 feed (Fig. 8), recorded at increasing temperatures in the range of 250 – 400°C, showed absorption bands in the range 1700 – 1300 cm^{-1} that were typical for the presence of the reaction products (i.e., CH_xO_y species).[26]

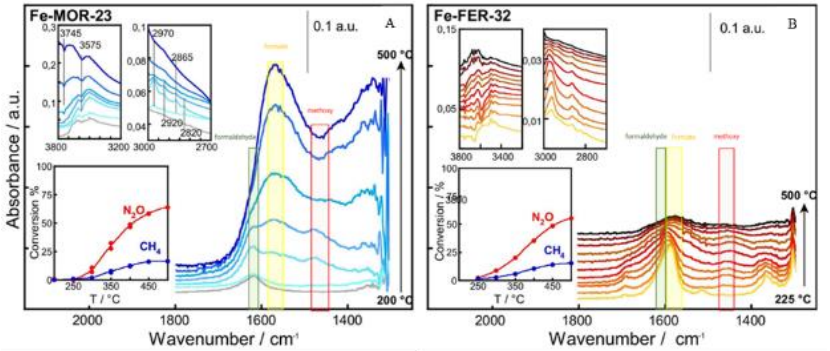

Fig. 8. Operando FTIR spectra of surface species during CR_{N2O} reaction at temperatures increasing up to 500°C: (A) Fe-MOR-23; and (B) Fe-FER-32 catalysts. The insets show the corresponding reactant conversions as a function of temperature and magnifications of the O-H and C-H regions.

The newly formed bands were assigned to formaldehyde (1620 cm^{-1}), formate (1590 – 1560 and 1390 cm^{-1}), and methoxy (1475 – 1435 cm^{-1}) species.[26] The CH_xO_y species were better defined in the experiments over Fe-FER-32, which probably indicates the lower heterogeneity of these surface species. This finding clearly suggests that the topology influenced the type of intermediate species. However, the CHxOy species were more abundant over Fe-MOR-23 than over Fe-FER-32, although both Fe-MOR-23 and Fe-FER-32 exhibited rather similar catalytic activity. These differences in the population of CH_xO_y and the catalytic activity of the studied Fe-zeolites can tentatively be assigned to the presence of a higher fraction of spectator species in the case of Fe-MOR-23 compared to Fe-FER-32.

Analysis of the operando FTIR results during SCR_{N2O} revealed the formation of formaldehyde and formate species (Fig 9). Compared with the CR_{N2O} conditions, the FTIR spectra for Fe-FER-32 and Fe-MOR-23 under SCR_{N2O} conditions were free from methoxy species. These findings indicate that the addition of O_2 to the reaction mixture blocked the formation (or accumulation) of methoxy species on the surface. A similar amount of CH_xO_y (formaldehyde and formate species) was observed on the Fe-FER-32 sample in both the CR_{N2O} and SCR_{N2O} reactions.

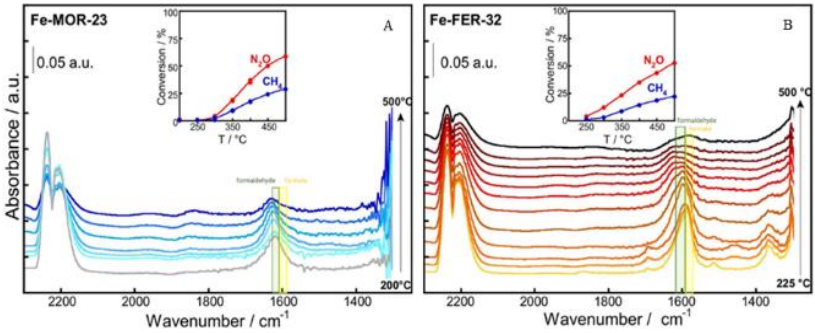

Fig. 9. Operando FTIR spectra of surface species during SCR_{N2O} reaction at temperatures increasing up to 500°C: (A) Fe-MOR-23; and (B) Fe-FER-32 catalysts. The insets show the corresponding reactant conversions as a function of temperature, and magnifications of the O-H and C-H regions.

The results presented above clearly show that the FER and MOR matrices, with comparable amounts of Al pairs, influenced the formation of individual Fe(II) sites with different redox properties. Accordingly, the differences in zeolite topology affected the formation of various types of Fe species with different valencies. It was confirmed that the Fe-FER was more active than the Fe-MOR in the reduction of N_2O in the presence of O_2 (SCR_{N2O}), whereas both systems were similarly active for CR_{N2O}. A combination of structural characteristics of the Fe-MOR and Fe-FER samples, with their catalytic performance, revealed that, in the CR_{N2O} reaction, the active centers were Fe(II) located in cationic positions. In the case of SCR_{N2O}, the reaction conditions influenced the redox properties of the Fe species present in the Fe-FER and Fe-MOR samples.

IV Conclusions

The conclusions of the study are presented as answers to the questions posed in the aims of the thesis.

1. How to analyze the O_2 activation and following CH_4 oxidation over Fe-FER using spectroscopic techniques? The methodology used to explore the formation of α-O from O_2 splitting via Fe-FER was developed using in-situ Mössbauer, XANES, and FTIR spectroscopy. The structural and valence changes in Fe(II)→Fe(III) occurring over the β site in the Fe-FER was revealed by in-situ Mössbauer and XANES spectroscopy before and after O_2 interaction. Thus, the in-situ Mössbauer spectral benchmark of the α-O originating from O_2 stabilized on Fe in the FER was established. It was shown that the formation, kinetics, and oxidation properties of α-O can be analyzed using the in-situ FTIR technique in the region of the OH and T–O–T vibrations. Methane was used as a probe molecule to analyze the oxidation properties of α-O, and it was confirmed that the CH_4 was oxidized by α-O to methanol.

2. Do TMI ions other than Fe(II) ions form binuclear centers in FER for O_2/N_2O cleavage? The outcomes of FTIR spectroscopy and the DFT modeling confirmed that the FER topology is an optimal candidate for stabilizing divalent (TMI) cations in β cationic positions, which can form binuclear centers. Preparation of Co-, Ni-, and Mn-FERs with a high level of loading of bare divalent cations are feasible for all of these cations. Moreover, for the first time, the values of the FTIR extinction coefficients of the individual bare M(II) cations (M = Co, Ni, and Mn) located in the FER matrix were established.

3. Could zeolites of topologies other than FER stabilize Fe(II) binuclear active centers for O_2 splitting? The results of the DFT calculations indicated that the binuclear Fe(II) sites could be accommodated in MOR, *BEA, and LTA. However, the DFT calculations revealed that the splitting of O_2 over Fe(II) zeolites was significantly influenced by the location of the Fe centers and their mutual orientations. The optimal parallel orientation of Fe(II) centers in the MOR and *BEA zeolites enabled the splitting of O_2, whereas the non-parallel orientation of Fe binuclear centers in the LTA zeolite precluded O_2 cleavage. The results of this study have confirmed that the capability for O_2 splitting represents a general property of the binuclear Fe(II) centers stabilized in zeolites.

4. Does the α-O originating from N_2O and O_2 splitting stabilized on the binuclear centers of Co(II), Ni(II), Fe(II) and Mn(II) in FER zeolites react with CH_4 at low temperatures? The findings obtained from FTIR and mass spectrometry analysis confirmed that the α-O species was formed by O_2/N_2O cleavage over the binuclear Ni(II), Mn(II), Fe(II), and Co(II) in the FER reacting with CH_4, oxidizing it to methanol at RT. The methanol produced over distant binuclear cationic structures in FER zeolites was released to the gas phase without using an effluent.

5. How is the cation speciation in FER and MOR zeolites reflected in the catalytic performance of Fe-zeolites in the CR_{N2O} and SCR_{N2O} of N_2O by CH_4? Our findings showed that FER and MOR matrices with a comparable amount of Al pairs stabilized the Fe(II) sites with different redox properties. Fe-FER zeolite contained a higher fraction of well-defined Fe(II) than its Fe-MOR analog with similar Fe loading. The Fe-FER zeolite was also a more active catalyst than the Fe-MOR in the SCR_{N2O} of

N_2O by CH_4, whereas both systems were similarly active for CR_{N2O}. A combination of the structural characteristics of the Fe-MOR and Fe-FER zeolites with their catalytic performance revealed that, in the CR_{N2O} reaction, the active centers were Fe(II) located in cationic positions. In the case of the SCR_{N2O}, the reaction conditions influenced the redox properties of the Fe species present in both the Fe-FER and Fe-MOR zeolites.

V List of references

(1) Corma, A. *Chem. Rev.* **1995,** 95(3), 559−614.

(2) Zhang, Q.; Yu, J. H.; Corma, A. *Adv. Mater.* **2020,** 32(44), 2002927.

(3) Tabor, E.; Bernauer, M.; Wichterlova, B.; Dedecek, J. *Catal. Sci. Technol.* **2019,** 9(16), 4262−4275.

(4) Li, C. G.; Vidal-Moya, A.; Miguel, P. J.; Dedecek, J.; Boronat, M.; Corma, A. *ACS Catal.* **2018**, 8(8), 7688–7697.

(5) Dedecek, J.; Sobalik, Z.; Wichterlova, B. *Catal. Rev.* **2012**, 54(2), 135–223.

(6) Sobalik, Z.; Dedecek, J.; Ikonnikov, I.; Wichterlova, B. *Micropor. Mesopor. Mater.* **1998**,
21(4-6), 525–532.

(7) Dedecek, J.; Wichterlova, B. *J. Phys. Chem. B.* **1999**, 103(9), 1462–1476.

(8) Zhao, G.; Drewery, M.; Mackie, J.; Oliver, T.; Kennedy, E. M.; Stockenhuber, M. *Energy Technol.* **2020**, 8(8), 1900665.

(9) https://www.epa.gov/gmi/importance-methane.

(10) Olivos-Suarez, A. I.; Szécsényi, A.; Hensen, E. J. M.; Ruiz-Martinez, J.; Pidko, E. A.; Gascon, J. *ACS Catal*. **2016**, 6, 2965−2981.

(11) Raynes, S.; Shah, M. A.; Taylor, R. A. *Dalton Trans*. **2019**, 48(28), 10364–10384.

(12) Sushkevich, V. L.; Verel, R.; van Bokhoven, J. A. *Angew. Chem. Int. Ed.* **2020**, 59(2), 910–918.

(13) Panov, G. I.; Sobolev, V. I.; Kharitonov, A. S. *J. Mol. Catal*. **1990**, 61(1), 85–97.

(14) Jisa, K.; Novakova, J.; Schwarze, M.; Vondrova, A.; Sklenak, S.; Sobalik, Z. *J. Catal*. **2009**, 262(1), 27–34.

(15) Snyder, B. E. R. et al. *Nature*. **2016**, 536(7616), 317.

(16) Bols, M. L.; Hallaert, S. D.; Snyder, B. E. R.; Devos, J.; Plessers, D.; Rhoda, H. M.; Dusselier, M.; Schoonheydt, R. A.; Pierloot, K.; Solomon, E. I.; Sels, B. F. *J. Am. Chem. Soc.* **2018**, 140(38), 12021–12032.

(17) Tsai, M. L.; Hadt, R. G.; Vanelderen, P.; Sels, B. F.; Schoonheydt, R. A.; and Solomon, E. I. *J. Am. Chem. Soc.* **2014**, 136, 3522–3529.

(18) Zhang, X.; Shen, Q.; He, C.; Ma, C.; Cheng, J.; Liu, Z.; and Hao, Z. *Catal. Sci. Technol.* **2012**, 2, 1249–1258.

(19) Ravi, M.; Ranocchiari, M.; van Bokhoven, J. A. *Angew. Chem. Int. Ed.* **2017**, 56(52), 16464–16483.

(20) Mahyuddin, M. H.; Yoshizawa, K. *Catal. Sci. Technol.* **2018**, 8, 5875–5885.

(21) Beznis, N. V.; Weckhuysen, B. M.; Bitter, J. H. *Catal. Lett.* **2010**, 136, 52–56.

(22) Tabor, E.; Dedecek, J.; Mlekodaj, K.; Sobalik, Z.; Andrikopoulos, P. C.; Sklenak, S. *Sci. Adv.* **2020**, 6(20), eaaz9776.

(23) Sklenak, S.; Andrikopoulos, P. C.; Boekfa, B.; Jansang, B.; Novakova, J.; Benco, L.; Bucko, T.; Hafner, J.; Dedecek, J.; Sobalik, Z. *J. Catal.* **2010**, 272(2), 262–274.

(24) Sushkevich, V. L.; van Bokhoven, J. A. *Catal. Sci. Technol.* **2020**, 10, 382−390.

(25) Sobalik, Z.; Tvaruzkova, Z.; Wichterlova, B. *J. Phys. Chem. B.* **1998,** (102), 1077.

(26) Nobukawa, T.; Yoshida, M.; Kameoka, S.; Tomishige, K.; Kunimori, K. *J. Phys. Chem. B*. **2004**, 108(13), 4071–4079.

(27) Busca, G.; Elmi, A. S.; Forzatti, P. *J. Phys. Chem.* **1987**, 91(20), 5263–5269.

(28) Berlier, G.; Zecchina, A.; Spoto, G.; Ricchiardi, G.; Bordiga, S.; Lamberti, C. *J. Catal.* **2003**, 215(2), 264–270.

VI List of published works

1. **Mariia Lemishka**, Jiri Dedecek, Kinga Mlekodaj, Zdenek Sobalik, Stepan Sklenak, Edyta Tabor. Speciation and siting of divalent transition metal ions in silicon-rich zeolites. An FTIR study. *Pure and Applied Chemistry*. 2019, 91(11), 1721–173.

2. Edyta Tabor, **Mariia Lemishka**, Zdenek Sobalik, Kinga Mlekodaj, Prokopis C. Andrikopoulous, Jiri Dedecek, Stepan Sklenak. Low-temperature selective oxidation of methane over distant binuclear cationic centers in zeolites. *Communications Chemistry*. 2019, 2, 71.

3. Kinga Mlekodaj, **Mariia Lemishka**, Stepan Sklenak, Jiri Dedecek, Edyta Tabor. Dioxygen splitting at room temperature over distant binuclear transition metal centers in zeolites for direct oxidation of methane to methanol. *Chemical Communication*. 2021, 57, 3472–3475.

4. Edyta Tabor, **Mariia Lemishka**, Joanna E. Olszowka, Kinga Mlekodaj, Jiri Dedecek, Prokopis C. Andrikopoulos, and Stepan Sklenak. Splitting Dioxygen over Distant Binuclear Fe Sites in Zeolites. Effect of the Local Arrangement and Framework Topology. *ACS Catalysis*. 2021, 11, 4, 2340–2355.

5. Kinga Mlekodaj, **Mariia Lemishka**, Agnieszka Kornas, Dominik K. Wierzbicki, Joanna E. Olszowka, Hana Jirglová, Jiri Dedecek, and Edyta Tabor. Evolution of Active Oxygen Species Originating from O_2 Cleavage over Fe-FER for Application in Methane Oxidation. *ACS Catalysis*. 2023, 13, 3345–3355.

6. Maria Cristina Campa, Daniela Pietrogiacomi, Carlotta Catracchia, Simone Morpurgo, Joanna Olszowka, Kinga Mlekodaj, **Mariia Lemishka**, Jiri Dedecek, Agnieszka Kornas, Edyta Tabor. Fe-MOR, and Fe-FER as catalysts for abatement of N_2O with CH_4: in situ UV-vis DRS and operando FTIR study. *Applied Catalysis B: Environmental*. 2024, 342, 123360.